Thalamic energy dysfunction is associated with thalamo-cortical tract damage in multiple sclerosis: a diffusion spectroscopy study

Journal:	*Multiple Sclerosis Journal*
Manuscript ID	MSJ-19-0909.R1
Manuscript Type:	Original Research Paper
Date Submitted by the Author:	n/a
Complete List of Authors:	Ricigliano, Vito; Sorbonne Université, UPMC Paris 06, Institut du Cerveau et de la Moelle épinière (ICM), Paris, France, UPMC Paris 06 Tonietto, Matteo; Sorbonne Université, UPMC Paris 06, Institut du Cerveau et de la Moelle épinière (ICM), Paris, France, UPMC Paris 06 Palladino, Raffaele; Imperial College London Department of Primary Care and Public Health, Department of Primary Care and Public Health Poirion, Emilie; Sorbonne Université, UPMC Paris 06, Institut du Cerveau et de la Moelle épinière (ICM), Paris, France, UPMC Paris 06 De Luca, Alberto; University Medical Center Utrecht, Image Sciences Institute Branzoli, Francesca; Institut du Cerveau et de la Moelle épinière (ICM), Paris, France , Centre de NeuroImagerie de Recherche Bera, Geraldine; Sorbonne Universités, UPMC Paris 06, Institut du Cerveau et de la Moelle épinière, ICM, Hôpital de la Pitié Salpêtrière, Inserm UMR S 1127, CNRS UMR 7225, Institut du Cerveau et de la Moelle épinière Maillart, Elisabeth; Hopital Universitaire Pitie Salpetriere, Neurology; Stankoff, Bruno; APHP, St Antoine Hospital, Neurology Department Bodini, Benedetta; Centre de recherche du cerveau et de la moelle ép Pierre and Marie Curie University Paris, France, Sorbonne Universités, UPMC Paris 06, Institut du Cerveau et de la Moelle épinière, ICM, Hôpital de la Pitié Salpêtrière, Inserm UMR S 1127, CNRS UMR 7225
Keywords:	Multiple sclerosis, energy dysfunction, diffusion-weighted spectroscopy, diffusion tensor imaging, tractography, neurodegeneration
Abstract:	Background:Diffusion-weighted 1H magnetic resonance spectroscopy (DW-MRS) allows to quantify creatine-phosphocreatine brain diffusivity (ADC(tCr)), whose reduction in multiple sclerosis (MS) has been

	proposed as a proxy of energy dysfunction. Objective:To investigate whether thalamic ADC(tCr) changes are associated with thalamo-cortical tract damage in MS. Methods:Twenty patients with MS and thirteen healthy controls (HC) were enrolled in a DW-MRS and DW imaging (DWI) study. From DW-MRS, ADC(tCr) and total N-acetyl-aspartate diffusivity (ADC(tNAA)) were extracted in the thalami. Three thalamo-cortical tracts and one non-thalamic control tract were reconstructed from DWI. Fractional anisotropy (FA), mean (MD), axial (AD) and radial diffusivity (RD), reflecting microstructural integrity, were extracted for each tract. Associations between thalamic ADC(tCr) and tract metrics were assessed using linear regression models adjusting for age, sex, thalamic volume, thalamic ADC(tNAA) and tract-specific lesion load. Results:Lower thalamic ADC(tCr) was associated with higher MD and RD of thalamo-cortical projections in MS (MD:p=0.029; RD:p=0.017), but not in HC (MD:p=0.625, interaction term between thalamic ADC(tCr) and group=0.019; RD:p=0.320, interaction term=0.05). Thalamic ADC(tCr) was not associated with microstructural changes of the control tract. Conclusion:Reduced thalamic ADC(tCr) correlates with thalamo-cortical tract damage in MS, showing that pathologic changes in thalamic energy metabolism are associated with structural degeneration of connected fibers.

TITLE PAGE

Title: Thalamic energy dysfunction is associated with thalamo-cortical tract damage in multiple sclerosis: a diffusion spectroscopy study

Authors: Vito AG Ricigliano[1], Matteo Tonietto[1], Raffaele Palladino[2,3], Emilie Poirion[1], Alberto De Luca[4], Francesca Branzoli[1,5], Geraldine Bera[1], Elisabeth Maillart[6], Bruno Stankoff[1,7], Benedetta Bodini[1,7].

Affiliations:

[1]Sorbonne Universites, UPMC Paris 06, Institut du Cerveau et de la Moelle épinière (ICM), Paris, France,

[2]Department of Primary Care and Public Health, School of Public Health, Imperial College of London, UK

[3]Department of Public Health, University "Federico II" of Naples, Italy,

[4]Image Sciences Institute, University Medical Center Utrecht, The Netherlands,

[5]Centre de NeuroImagerie de Recherche - Institut du Cerveau et de la Moelle épinière (ICM), Paris, France

[6]Hopital De La Pitie Salpetriere, Paris, France

[7]APHP, St Antoine Hospital, Neurology Department, Paris, France

Keywords: 1) multiple sclerosis; 2) energy dysfunction; 3) diffusion-weighted spectroscopy; 4)

diffusion tensor imaging; 5) tractography; 6) neurodegeneration.

Corresponding Author: Benedetta Bodini, MD, PhD

Contact: Institut du Cerveau et de la moelle épinière, ICM, Sorbonne Université, UPMC Paris 06, UMR S 1127, and CNRS UMR 7225, Hopital Pitié-Salpêtrière, 75013, Paris, France.

E-mail: benedetta.bodini@aphp.fr Tel: +33 1 57 27 44 63 Fax: +33 1 42 16 57 64

ABSTRACT

Background: Diffusion-weighted ^{1}H magnetic resonance spectroscopy (DW-MRS) allows to quantify creatine-phosphocreatine brain diffusivity (ADC(tCr)), whose reduction in multiple sclerosis (MS) has been proposed as a proxy of energy dysfunction.

Objective: To investigate whether thalamic ADC(tCr) changes are associated with thalamo-cortical tract damage in MS.

Methods: Twenty patients with MS and thirteen healthy controls (HC) were enrolled in a DW-MRS and DW imaging (DWI) study. From DW-MRS, ADC(tCr) and total N-acetyl-aspartate diffusivity (ADC(tNAA)) were extracted in the thalami. Three thalamo-cortical tracts and one non-thalamic control tract were reconstructed from DWI. Fractional anisotropy (FA), mean (MD), axial (AD) and radial diffusivity (RD), reflecting microstructural integrity, were extracted for each tract. Associations between thalamic ADC(tCr) and tract metrics were assessed using linear regression models adjusting for age, sex, thalamic volume, thalamic ADC(tNAA) and tract-specific lesion load.

Results: Lower thalamic ADC(tCr) was associated with higher MD and RD of thalamo-cortical projections in MS (MD:p=0.029; RD:p=0.017), but not in HC (MD:p=0.625, interaction term between thalamic ADC(tCr) and group=0.019; RD:p=0.320, interaction term=0.05). Thalamic ADC(tCr) was not associated with microstructural changes of the control tract.

Conclusion: Reduced thalamic ADC(tCr) correlates with thalamo-cortical tract damage in MS, showing that pathologic changes in thalamic energy metabolism are associated with structural degeneration of connected fibers.

INTRODUCTION

In multiple sclerosis (MS), the mechanisms underlying the neurodegenerative component of the disease remain poorly understood.[1]

Several pathways have been suggested to drive neurodegeneration, including demyelination, excitotoxicity, ion channel dysfunction and oxidative stress, each potentially inducing a condition of energy dysregulation.[2] Sodium channel redistribution and mitochondrial dysfunction in demyelinated axons produce early adaptive changes which result in neurons entering into a "virtual hypoxia" state.[3] This condition is characterized by increased energy demand coupled with insufficient supply which, if not reversed, lead to permanent energy deprivation and irreversible degeneration.[4]

Diffusion-weighted ^{1}H magnetic resonance spectroscopy (DW-MRS) integrates metabolic information from classical MRS together with measures of molecular displacement via magnetic field gradients for diffusion sensitization.[5] In a recent study using DW-MRS, we showed a decrease in the diffusivity of creatine+phosphocreatine (total creatine, tCr) - a tandem of metabolites involved in adenosine triphosphate production - in the thalami and the corona radiata in MS.[6] With some caution, this lower tCr diffusivity was interpreted as a proxy of energy dysregulation as it could result from the relative increase of the heavier and less diffusible PCr (phosphocreatine) fraction, whose consumption is diminished in MS due to impaired creatine kinase activity.[7] Interestingly, this reduced tCr diffusivity was shown to be independent of neuro-axonal damage, measured by the concentration and diffusivity of total N-acetyl-aspartate (tNAA).[6]

The thalamus is a highly interconnected brain hub extensively involved in MS pathology.[8] Previous studies have demonstrated a quantitative correlation between thalamic tissue loss and microstructural changes affecting thalamo-cortical tracts, suggesting the interdependence of grey matter (GM) atrophy and white matter (WM) damage in this disease.[9,10]

Building up on our results, we questioned here whether reduced thalamic diffusivity of metabolites related to energy production, which is thought to reflect energy dysregulation and possibly precede irreversible neuro-axonal degeneration,[6] is already associated with (and therefore potentially responsible for) microstructural damage of connected thalamo-cortical projections, independently of thalamic volume.

To test this hypothesis, we combined DW-MRS and diffusion tensor imaging (DTI) in a group of patients with MS and a group of age- and sex-matched healthy controls (HC).

METHODS

Subjects

Imaging and clinical data were collected for twenty-five patients with MS (17 relapsing-remitting [RRMS] and 8 progressive [PMS]) according to the 2010 revised McDonald criteria[11] (15 women, mean age = 46.1 years, standard deviation [SD] = 13.9) and 18 HC (9 women, mean age = 41.1 years, SD = 12.2).[6] All subjects were enrolled at the Centre of Clinical Investigation, Pitié-Salpêtrière hospital (Paris, France) between November 2014 and March 2015. Inclusion criteria for all subjects: (i) age 18-65 years; ii) being able to understand the study objective and procedure; (iii) efficient contraception for women of potential child-bearing; (iv) inscription to the national health care system; (v) having signed the written consent form. Additionally, for HC: no evolutive pathology or positive history of any neurological/psychiatric disorders. For patients, no limitations of disease duration was set and all lines of disease-modifying treatments (DMT) of MS were allowed. No patients with other neurological diseases different than MS were included in the study. In this original cohort, good quality DTI data were not available for 5 patients and 5 HC, reducing the suitable data for this specific study to a total of 20 patients (14 RRMS, 4 secondary and 2 primary PMS) and 13 HC. All participants provided written informed consent and the study was approved by the local ethic committee.

MRI/MRS acquisition

Images were acquired on a Siemens 3T MAGNETOM Trio system with 40mT/m maximum gradient strength and a 32-channel receive-only head coil. Acquired sequences included: i) a three-dimensional T1-weighted (T1-w) magnetization prepared rapid gradient echo; ii) a two-dimensional turbo spin echo T2-weighted and a T2 fluid attenuated inversion recovery (FLAIR); iii) a single-voxel, PRESS sequence

combined with bipolar diffusion gradients for DW-MRS acquisition.[12] In particular, a 23(AP)×18(FH)×30(LR)mm^3 volume of interest (VOI) was placed in the bilateral thalami (Figure 1) and visually checked by a DW-MRS expert (F.B.) to include the whole thalamus, with minor positional adjustments from one subject to another; and iv) a multi-slice 2D spin-echo planar sequence for DW imaging. Sequence parameters are detailed in Supplementary S1.

MRI post-processing

In patients, WM lesions were manually segmented on T2-w images with reference to FLAIR images using Jim (v7.0, http://www.xinapse.com/j-im-7-software/), and then aligned to T1-w images using a rigid registration. After lesion filling, the T1-w volumes were processed with FIRST, part of FSL (v5.0.10, https://fsl.fmrib.ox.ac.uk/fsl/fslwiki/), to segment the thalami and compute the thalamic volume normalized by the brain parenchymal fraction (NTV). Segmentation of cortical GM and parcellation of individual thalamic nuclei was performed on T1-w volumes using the development version of Freesurfer.[13]

DW images were preprocessed in ExploreDTI (v4.8.6, http://www.exploredti.com/),[14] including motion, eddy current and EPI distortion corrections by non-linear registration to the T1-w image. The following step was the robust fit[15] of the tensor and the calculation of maps of fractional anisotropy (FA), mean diffusivity (MD), radial and axial diffusivity (AD and RD).

Whole deterministic brain tractography was calculated in ExploreDTI using the constrained spherical deconvolution approach with a maximum angle threshold of 30°, step-size 1 mm, FOD threshold 0.1.[16]

From the whole brain tractography, already aligned with the corresponding T1-w scan, virtual *in vivo*

dissections of tracts were performed in each subject feeding TrackVis (v0.6.1, http://trackvis.org/)[17] with manually drawn regions-of-interest (ROIs).[18] Three thalamo-cortical tract pairs – the right and left somatosensory tract (SS), optic radiation (OR) and prefrontal tract (PF) (Figure 2a-c) – and one control tract pair unconnected to the thalamus – the right and left arcuate fasciculus (AF) (Figure 2d) – were dissected as detailed in Supplementary S2. All the ROIs were placed by a neurologist trained in tractography and tracts were confirmed visually for anatomic accuracy based on published atlases.[18] The impact of WM lesions on fiber tracking was visually checked to verify that lesions were not systematically omitted during tractography or did not induce interruptions/distortions in the fiber orientation reconstruction algorithm.[19] All fibers passing through the defined ROIs were reconstructed in three dimensions and undesired streamlines were excluded through the placement of exclusion ROIs.[18] The volume of each tract was extracted from TrackVis and expressed in milliliters.

In each subject, the mean values of FA, MD, AD and RD were extracted from each of the 2 tract masks of the three thalamo-cortical tract pairs (right and left SS, right and left OR, right and left PF) and of the control tract pair (right and left AF). To account for left-right asymmetries in tract volume (e.g due to manual dominance), the mean of each DTI-derived metric for each tract pair was calculated taking into account the weight of tract volume, as follows: (DTI-derived metric of the right tract x volume of the right tract + DTI-derived metric of the left tract x volume of the left tract)/(volume of the right tract + volume of the left tract).

The lesion load relative to each tract was calculated overlaying binary masks of WM lesions on T1-w images onto the tracts dissected in TrackVis. This automatically returned the proportion of tract voxels overlapping with lesional voxels, and was expressed as the percentage of tract volume occupied by

lesions.

MRS post-processing

Phase and frequency drift corrections were performed for individual spectra before summation in MATLAB. Eddy current corrections were based on the phase information from non-water-suppressed spectra. Quantification of spectral data was performed with LCModel.[20] The apparent diffusion coefficient (ADC) of tCr was extracted from the thalamic VOI as the slope of the logarithm of the signal decay induced by diffusion weighting, as previously described.[6] The ADC of another metabolite (tNAA) was also extracted from the thalamic VOI.[6] To account for partial volume effect of WM tissue inside the DW-MRS voxel, the DW-MRS VOI was overlayed onto the segmented thalami on the T1-w volumes, and a GM/WM ratio inside the DW-MRS voxel was extracted for each subject. This overlaying step also allowed to verify that all the selected thalamic nuclei were included in the thalamic DW-MRS VOI.

Simulation of ADC(tCr) changes for different PCr/Cr ratios

The relative contribution of Cr and PCr concentration to ADC(tCr) was calculated using a mathematical simulation of the normalized signal decay of tCr as a function of the b-value for different PCr/Cr concentration ratios (Supplementary S3).

Statistical analysis

Group differences between patients with MS and HC in age, sex and NTV were evaluated with Wilcoxon rank-sum test (for age and NTV) and Fisher's exact test (for sex).

Differences in mean thalamic ADC(tCr) between patients with MS and HC were assessed employing linear regression models adjusted for age, sex and NTV.

To test for differences between patients with MS and HC in mean DTI-derived metrics, a "pooled analysis" of the four tract pairs (3 thalamo-cortical tract pairs and 1 control tract pair) was run through linear mixed effect regression models, accounting for the hierarchical structure of the data (i.e., each subject contributing with four measurements) and adjusting for age, sex and single tract.

To further assess the impact of WM lesions on thalamic volumes, DTI and MRS-derived metrics in patients with MS, linear regression models adjusted for age and sex were used to test the association between: i) total WM lesion volume and NTV; ii) left/right tract-specific lesion load in and the volumes of the corresponding ipsilateral thalamic nuclei (ventroposterolateral nucleus [VPLN] for the SS, mediodorsal nucleus [MDN] for the PF, lateral geniculate nucleus [LGN] for the OR); iii) tract-specific lesion load and DTI-derived metrics of tracts; iv) tract-specific lesion load and thalamic ADC(tCr). Analyses were performed on the whole group of patients with MS, as well as on the RRMS (n=14) and PMS (n=6) subgroups.

To define whether thalamic energy dysfunction was associated with the microstructural damage of the 3 thalamo-cortical tract pairs in patients only and independently of NTV, we used a two-step approach. First, we fitted two separate linear mixed effect models, one in patients and one in HC, to test the association between thalamic ADC(tCr) and each of the 4 DTI-derived metrics (FA, MD, AD and RD) of the 3 thalamo-cortical tracts (SS, OR, and PF) in a "pooled analysis". All models accounted for the hierarchical structure of the data, and were adjusted for single tracts, age, sex, NTV, and tract-specific lesion load (in patients only). To adjust for the diffusivity of metabolites other than tCr, thalamic ADC(tNAA) was also included in the model as confounding variable. Then, to establish whether the associations tested separately in patients and HC were significantly different between the 2 groups, we

used a linear mixed effect model including an interaction term between thalamic ADC(tCr) and subject group (patients/HC), adjusting for single tracts, NTV, thalamic ADC(tNAA), age and sex.

Finally, to assess whether the association between thalamic ADC(tCr) and DTI-derived metrics was specific for thalamo-cortical projections or also extended to tracts unconnected to the thalamus, the association was separately tested for each of the three thalamo-cortical tracts and for the control tract (AF) by univariate linear regression models.

All statistical analyses were performed with STATA (v14.0, https://www.stata.com/), considering $p<0.05$ as significant.

RESULTS

Demographic and imaging data

Patients with MS and HC did not significantly differ in terms of age and sex (p=0.407, and p=0.239, respectively), but patients had 8.4% (p=0.008) lower NTV compared to HC (Table 1)~~, as already observed in the original cohort.[6]~~ A significantly lower FA (-0.02, p<0.001), and a higher MD (0.61 m^2/s $x10^{-10}$, p<0.001), AD (0.55 m^2/s $x10^{-10}$, p<0.01), and RD (0.65 m^2/s $x10^{-10}$, p<0.001) were found in patients compared to HC in the 4 analyzed tracts (SS, OR, PF and AF). Lesion load ranges for each tract spanned from 0 to 42.2% of tract volume (mean 7.29%)(Table 1).

Thalamic ADC(tCr) in MS: a proxy of energy dysregulation

Patients with MS showed significantly lower thalamic tCr diffusivity (-0.29 m^2/s $x10^{-10}$, p<0.001) than HC. Using a mathematical simulation to test whether the reduced tCr diffusivity could be the consequence of an unbalance of PCr/Cr concentrations, we found that the signal intensity/baseline (S/S_0) ratio increased from 0.56 to 0.59 when changing the PCr/Cr ratio from 1 to 4. (Supplementary Material S3). This resulted in an estimated ADC(tCr) drop from 0.19 µm2/ms to 0.17 µm2/ms, which corresponds to a 10% decrease, a bit lower than that observed in our study (17%).

WM lesion load is associated with DTI-derived metrics of tracts, but not with thalamic volumes and thalamic ADC(tCr) in MS

Tract-specific lesion load was correlated with all four DTI-derived metrics on the whole group and on the RRMS group (p<0.005 in all cases), and with MD, AD, RD on the PMS group (MD, AD, RD: P<0.005; FA: p=0.068).

No association was found between total WM lesion burden and NTV (coeff: -0.00001, p=0.12) or

between tract-specific lesion load of tracts and the corresponding ipsilateral thalamic nuclear volumes, separately assessed on the left and the right side (left: ventroposterolateral nucleus [VPLN]-SS: p=0.689; mediodorsal nucleus [MDN]-PF: p=0.644; lateral geniculate nucleus [LGN]-OR: p=0.184; right: VPLN-SS: p=0.430; MDN-PF: p=0.249; LGN-OR: p=0.069). No significant associations were found in subgroup analyses on RRMS or PMS. When testing the correlation between tract-specific lesion load and thalamic ADC(tCr), no association was identified, both in the whole group and in subgroup analyses (whole group: p=0.206; RRMS: p=0.712; PMS: p=0.815).

Thalamic ADC(tCr) is associated with thalamo-cortical tract damage in MS but not in HC

In patients with MS, lower thalamic ADC(tCr) was associated with lower FA, and higher MD and RD of the 3 thalamo-cortical tracts (SS, OR and PF), reflecting microstructural damage, after adjusting for age, sex, NTV, thalamic ADC(tNAA), single tracts and tract-specific lesions (FA: coeff:327.36, p=0.027; MD: coeff:-0.55, p=0.029; RD: coeff:-0.66, p=0.017). The associations between thalamic ADC(tCr) and AD was not significant (coeff:-0.34, p=0.158). In HC, no correlation was found between thalamic ADC(tCr) and DTI-derived metrics of the 3 thalamo-cortical tracts (SS, OR and PF) (FA: coeff:437.87, p=0.161; MD: coeff:-0.19, p=0.625; AD: coeff:0.34, p=0.407; RD: coeff:-0.46, p=0.320) (Figure 3 and Table 2).

The interaction model showed that the association between thalamic ADC(tCr) and DTI-derived metrics in connected thalamo-cortical tracts was significantly stronger in patients with MS compared to HC for MD, AD and RD (MD: interaction coefficient [IC]:-0.69, p=0.019; AD: IC:-0.78, p=0.008; RD: IC:-0.64, p=0.05), but not for FA (IC:177.57, p=0.328) (Table 2).

In MS, thalamic ADC(tCr) is associated with damage of thalamo-cortical tracts but not with that of the arcuate fasciculus

In patients with MS, single tract analysis of the 3 thalamo-cortical tracts confirmed the results obtained with the pooled analysis (Figure 4 and Table 3). In particular:

1) thalamic ADC(tCr) was correlated with MD and RD in all the 3 thalamo-cortical tracts;

2) thalamic ADC(tCr) was correlated with AD in 2 out of 3 thalamo-cortical tracts.

Single-tract analysis in HC showed that thalamic ADC(tCr) was not correlated with microstructural metrics in any of the thalamo-cortical tracts.

In the arcuate fasciculus, no association was found between thalamic ADC(tCr) and any microstructural metrics, neither in MS nor in HC.

DISCUSSION

Energy dysregulation has been proposed as a main contributor in the cascade of neurodegeneration in MS.[2-4] To explore its impact on tissue integrity, we focused on the diffusion properties of a key intermediate in ATP-generating reactions. In particular, we investigated *in vivo* the link between dysregulation of energy metabolism in the thalami, explored by DW-MRS, and microstructural damage of thalamo-cortical projections, measured with DTI.

As already shown,[6] patients with MS had decreased thalamic tCr diffusivity. This reduction could derive from the relative increase of the less diffusible PCr as compared to Cr. Indeed, several imaging studies have documented PCr accumulation relative to Cr reduction in MS.[7,21,22] To test this hypothesis, we performed a mathematical simulation of the normalized signal decay of tCr as a function of the b-value for different PCr/Cr concentration ratios. We found that the observed decrease in ADC(tCr) in MS was consistent with an increase of the PCr fraction as compared to Cr. Therefore, we interpreted the lower thalamic tCr diffusivity as a proxy of the ongoing energy dysregulation in MS.

When we tested the relationship between thalamic tCr diffusivity and the DTI-derived metrics of thalamo-cortical projections, we found the first *in vivo* evidence that a greater reduction of tCr diffusivity in the thalami, reflecting energy dysregulation in these deep GM regions, was associated with a more severe microstructural damage of connected tracts, as reflected by increased MD and RD. This association, which was found in the pooled analysis of all tracts taken together and confirmed in the single-tract analysis, was shown to be specific: i) at the disease level, as it was demonstrated in patients with MS, but not in HC; ii) at the spatial level, as it was selectively observed in tracts anatomically

connected to the thalamus, but not in the non-thalamic control tract; iii) at the metabolite level, as it was significant for ADC(tCr) independently of the diffusivity of a different metabolite in the same region (ADC(tNAA)).

A possible interpretation is that energy distress of thalamic neuronal cell bodies may spread towards the axons of connected tracts, ultimately being involved in their anterograde structural degeneration.[23,24] Indeed, following inflammation and demyelination, the neuron works at compensatory higher rhythms[25] to overcome the perturbations induced by altered transmembrane ion gradients and the changes in intracellular energy production. Dysfunctional mitochondrial energy supply could partly be compensated by the fast release of ATP from the Cr/PCr buffer, but these modifications may finally result in a persistent mismatch between energy demand and supply in the thalamic cell body.[3] This condition of energy dysregulation affects neuronal electrical discharge, structural protein synthesis and axonal transport, all crucially depending on cellular energy reserves.[26] Over time, if the energy distress is not reverted, the anterograde degeneration of the distal portion of the axon begins to unfold.[8] The hypothesis of an anterograde axonal damage is supported by *post mortem* data in MS showing that the levels of axonal motor proteins which are responsible for the anterograde transport are already reduced in the GM even before the appearance of demyelinated lesions.[24]

Though intriguing, this is only one of the possible explanations of the association between thalamic energy dysregulation and structural degeneration of thalamo-cortical fibers. An alternative hypothesis is that thalamic functional dysregulation is associated with connected tract pathology as a result of a damage primarily affecting WM axons. Primary WM changes could propagate along projection fibers[27] and induce a secondary injury in the connected neuronal cell bodies in the thalamus, resulting in an increased

energy distress in this region. Finally, our results could also reflect the combination of two independent pathological processes affecting simultaneously the deep GM and the connected WM tracts.[28] However, the cross-sectional nature of our study does not allow to define a univocal cause-and-effect relationship. Only longitudinal studies of large cohorts of patients could clarify which hypothesis, or which combination of hypotheses, best explains the relationship between thalamic energy dysregulation and thalamo-cortical tract damage in each clinical form of disease.

In our results, we found that WM lesion volume was not correlated with thalamic volume. Looking at this result tract-by-tract, tract-specific lesion load did not impact individual thalamic nuclear volumes or thalamic tCr diffusivity. These findings suggest that volumetric changes of individual thalamic nuclei and functional thalamic parameters are not simply explained by the lesion load in the corresponding thalamo-cortical tract. On the contrary, tract-specific lesion load is strongly correlated with DTI-derived metrics of tracts, as expected. This confirms the need to account for tract-specific lesions when testing the associations between energy and microstructural metrics. In pooled analysis, thalamic tCr diffusivity was associated with thalamo-cortical tract damage independently of tract-specific lesions, thalamic volumes and thalamic ADC(tNAA). With some caution, this may suggest that changes in thalamo-cortical WM tracts in MS may partly be the result of thalamic energy dysfunction *per se*, with a limited impact of thalamic cell loss and immune-mediated tissue destruction in WM lesions.[29] The component of axonal pathology developing independently of WM demyelination may be particularly relevant in the progressive phases of disease: previous neuropathological data have shown that irreversible neurodegenerative processes, developing at least in part outside visible lesions, are thought to be the underlying mechanisms of clinical progression.[30]

Some limitations have to be considered when interpreting our results. First, DW-MRS acquisitions have a low spatial resolution, and require the selection of a big voxel which suffers from partial volume contamination from proximal WM fibers. However, in our case, we believe that the impact of partial volume was limited, as the GM/WM ratios in the DW-MRS voxel were not statistically different between patients and HC (p=0.342). Another limitation related to DW-MRS is that we were able to measure tCr diffusivity but not the diffusivity of Cr and PCr separately. Therefore, only the direct experimental quantification of the diffusivity of the two separate fractions could help better define the biological meaning of the observed reduction in tCr diffusivity.

Thirdly, in our study mean MD and RD, but not FA, of thalamo-cortical projections were found to correlate with thalamic ADC(tCr) in MS versus HC in the interaction model. This could be due to the higher sensitivity of MD in detecting an early or spatially-limited microstructural damage in MS[31,32] or changes in free-water reflecting neuroinflammation.[33] Fourthly, due to the exploratory nature of this analysis, additional studies on larger cohorts should be performed to confirm our findings, in particular those at the single-tract level. Lastly, the measurement of tCr diffusivity by DW-MRS only gives a partial insight into the energy production mechanisms, in which the Cr/PCr buffer acts as an ancillary process.

Despite these limitations, our study provides novel insights into the relationship between deep GM energy dysfunction and WM microstructural damage in MS. A deeper understanding of the potential role of energy failure in driving structural neurodegeneration remains essential to develop effective neuroprotective strategies.[34]

DECLARATION OF CONFLICTING INTERESTS

The author(s) declared the following potential conflicts of interest with respect to the research, authorship, and/or publication of this article: V.A.G.R. has received travel grants from Novartis and Roche. M. T., R. P., A. D. L., E.P., F.B., G.B.: nothing to disclose. E. M. has received consulting and lecturing fees, travel grants from ad Scientiam, Biogen Idec, Genzyme, Novartis, Merck Serono, Roche, Sanofi, and Teva Pharma, and research support from Novartis and Roche. B. S. has received fees for advisory boards and lectures from Genzyme, Merck-Serono, Novartis, Teva and Biogen, and research support from Roche, Genzyme and Merck-Serono. B. B. has received research support from ARSEP, FISM and funding for traveling and/or speaker's honoraria from Novartis, Genzyme, Roche and Merck Serono.

FUNDING

The study was possible thanks to the support of the ARSEP and of the following grants: Institut des neuro-sciences translationnelle – ANR-10-IAIHU-06, and Infrastructure d'avenir en Biologie Santé – ANR-11-INBS-0006.

REFERENCES

1. Ontaneda D, Fox RJ, Chataway J. Clinical trials in progressive multiple sclerosis: Lessons learned and future perspectives. *Lancet Neurol* 2015; 14: 208-223.

2. Campbell GR, Worrall JT, Mahad DJ. The central role of mitochondria in axonal degeneration in multiple sclerosis. *Mult Scler* 2014; 20: 1806-1813.

3. Trapp BD, Stys PK. Virtual hypoxia and chronic necrosis of demyelinated axons in multiple sclerosis. *Lancet Neurol* 2009; 8: 280–291.

4. Friese MA, Schattling B, Fugger L. Mechanisms of neurodegeneration and axonal dysfunction in multiple sclerosis. *Nat Rev Neurol* 2014; 10: 225–238.

5. Palombo M, Shemesh N, Ronen I, Valette J. Insights into brain microstructure from in vivo DW-MRS. *Neuroimage* 2018; 182: 97-116.

6. Bodini B, Branzoli F, Poirion E, et al. Dysregulation of energy metabolism in multiple sclerosis measured in vivo with diffusion-weighted spectroscopy. *Mult Scler* 2018; 24: 313-321.

7. Steen C, Wilczak N, Hoogduin JM, Koch M, de Keyser J. Reduced creatine kinase B activity in multiple sclerosis normal appearing white matter. *PLoS ONE* 2010; 5: e10811.

8. Kipp M, Wagenknecht N, Beyer C, Samer S, Wuerfel J, Nikoubashman O. Thalamus pathology in multiple sclerosis: From biology to clinical application. *Cell Mol Life Sci* 2015; 72: 1127-1147.

9. Kolasinski J, Stagg CJ, Chance SA, et al. A combined post-mortem magnetic resonance imaging and quantitative histological study of multiple sclerosis pathology. *Brain* 2012; 135 (Pt 10): 2938–2951.

10. Bodini B, Khaleeli Z, Cercignani M, Miller DH, Thompson AJ, Ciccarelli O. Exploring the relationship between white matter and gray matter damage in early primary progressive multiple sclerosis: An in vivo study with TBSS and VBM. *Hum Brain Mapp* 2009; 30: 2852-2861.

11. Polman CH, Reingold SC, Banwell B, et al. Diagnostic criteria for multiple sclerosis: 2010 Revisions to the McDonald criteria. *Ann Neurol* 2011; 69: 292–302.

12. Ronen I, Valette J. Diffusion-weighted magnetic resonance spectroscopy. *EMagRes* 2015; 4: 733-750.

13. Iglesias JE, Insausti R, Lerma-Usabiaga G, et al. A probabilistic atlas of the human thalamic nuclei combining ex vivo MRI and histology. *Neuroimage* 2018; 183: 314-326.

14. Leemans A, Jeurissen B, Sijbers J, Jones DK. ExploreDTI: a graphical toolbox for processing, analyzing, and visualizing diffusion MR data. *Proc Intl Soc Mag Reson Med* 2009; 17: 3537.

15. Tax CMW, Otte WM, Viergever MA, Dijkhuizen RM, Leemans A. REKINDLE: Robust Extraction of Kurtosis INDices with Linear Estimation. *Magn Reson Med* 2015; 73: 794-808.

16. Tournier JD, Calamante F, Connelly A. Robust determination of the fibre orientation distribution in diffusion MRI: Non-negativity constrained super-resolved spherical deconvolution. *Neuroimage* 2007; 35: 1459-1472.

17. Wang R, Wedeen VJ. Diffusion Toolkit : A Software Package for Diffusion Imaging Data Processing and Tractography. *Proc Intl Soc Mag Reson Med* 2007; 15: 3720.

18. Catani M, Thiebaut de Schotten M. A diffusion tensor imaging tractography atlas for virtual in vivo dissections. *Cortex* 2008; 44: 1105-1132.

19. Lipp I, Parker GD, Tallantyre E, et al. Tractography in the presence of white matter lesions in multiple sclerosis. *Neuroimage* 2019; 209: 116471.

20. Provencher SW. Automatic quantitation of localized in vivo 1H spectra with LCModel. *NMR Biomed* 2001; 14: 260-264.

21. Kauv P, Ayache SS, Créange A, et al. Adenosine Triphosphate Metabolism Measured by Phosphorus Magnetic Resonance Spectroscopy: A Potential Biomarker for Multiple Sclerosis Severity. *Eur Neurol* 2017; 77: 316-321.

22. Hattingen E, Magerkurth J, Pilatus U, et al. Combined (1)H and (31)P spectroscopy provides new insights into the pathobiochemistry of brain damage in multiple sclerosis. *NMR Biomed* 2011; 24: 536-46.

23. Wood ET, Ronen I, Techawiboonwong A, et al. Investigating axonal damage in multiple sclerosis by diffusion tensor spectroscopy. J *Neurosci* 2012; 32: 6665-6669.

24. Hares K, Kemp K, Rice C, Gray E, Scolding N, Wilkins A. Reduced axonal motor protein expression in non-lesional grey matter in multiple sclerosis. *Mult Scler* 2014; 20: 812-821.

25. Campbell GR, Ohno N, Turnbull DM, Mahad DJ. Mitochondrial changes within axons in multiple sclerosis: An update. *Curr Opin Neurol* 2012; 25: 221-230.

26. Sasaki Y. Metabolic aspects of neuronal degeneration: From a NAD+ point of view. *Neurosci Res* 2019; 139: 9-20.

27. Huang-Link Y-M, Al-Hawasi A, Eveman I. Retrograde degeneration of visual pathway: hemimacular thinning of retinal ganglion cell layer in progressive and active multiple sclerosis. *J Neurol* 2014; 261: 2453-2456.

28. Bodini B, Chard D, Altmann DR, et al. White and gray matter damage in primary progressive MS - The chicken or the egg? *Neurology* 2016; 86: 170-176.

29. Brück W. Inflammatory demyelination is not central to the pathogenesis of multiple sclerosis. *J Neurol* 2005; 252 Suppl 5: v10-15.

30. Tallantyre EC, Bø L, Al-Rawashdeh O, et al. Clinico-pathological evidence that axonal loss underlies disability in progressive multiple sclerosis. *Mult Scler* 2010; 16: 406-411.

31. Koubiyr I, Deloire M, Coupé P, et al. Differential gray matter vulnerability in the 1 year following a clinically isolated syndrome. *Front Neurol* 2018; 9: 824.

32. Li HQ, Yin B, Quan C, et al. Evaluation of patients with relapsing-remitting multiple sclerosis using tract-based spatial statistics analysis: Diffusion kurtosis imaging. *BMC Neurol* 2018; 18: 108.

33. Pasternak O, Shenton ME, Westin C-F. Estimation of Extracellular Volume from Regularized Multi-shell Diffusion MRI. *Med Image Comput Comput Assist Interv* 2012; 15 (Pt 2): 305-312.

34. Vallée A, Lecarpentier Y, Guillevin R, Vallée JN. Demyelination in multiple sclerosis: Reprogramming energy metabolism and potential PPARγ agonist treatment approaches. *Int J Mol Sci* 2018; 19. pii:E1212.

Table 1

Clinical and radiological characteristics	Patients with MS	HC
number	20	13
age (years)	46.9±13.7	43.5±12.1
sex (female/male)	13/7	6/7
Disease duration (years)	7.3±5.9	-
EDSS, median (range)	3.5 (0-6)	-
T2 lesion load (cm^3)	30.6±26.1	-
Tract-specific lesion load, mean (range)†:		
Somatosensory tract	4.8 (0-12.5)	-
Optic radiations	15.7 (0-42.2)	-
Dorsolateral prefrontal tract	5.4 (0-17)	-
Arcuate fasciculus	3.2 (0-14.1)	-
Normalized thalamic volume (NTV)	11±0.9	12.1±0.9

Table 1. Demographic, clinical and radiological characteristics of patients with MS and healthy controls. Main characteristics of patients with MS and HC. Values are the mean ± standard deviation (SD) unless stated otherwise. EDSS: expanded disability status scale; cm^3: cubic centimeters. †= expressed as the percentage of tract volume occupied by lesions.

Table 2

Thalamic ADC(tCr)										
	MS				HC				interaction			
	coefficient	*95% CI*		*p*	*coefficient*	*95% CI*		*p*	*coefficient*	*95% CI*		*p*
FA	327.36	37.96	616.75	0.027*	437.87	-173.98	1049.72	0.161	177.57	-177.98	533.11	0.328
MD	-0.55	-1.05	-0.06	0.029*	-0.19	-0.97	0.59	0.625	-0.69	-1.26	-0.11	0.019*
AD	-0.34	-0.82	0.13	0.158	0.34	-0.46	1.14	0.407	-0.78	-1.35	-0.20	0.008*
RD	-0.66	-1.20	-0.12	0.017*	-0.46	-1.37	0.45	0.320	-0.64	-1.28	-0.00	0.050*

Table 2. Association between thalamic ADC(tCr) and microstructural metrics of thalamo-cortical tracts: pooled analysis. Correlations between thalamic ADC(tCr) and DTI-derived metrics (FA, MD, AD, RD) of thalamo-cortical tracts in patients with MS and HC, and interaction term for the between-group comparison. FA: fractional anisotropy; MD: mean diffusivity; AD: axial diffusivity; RD: radial diffusivity, ADC(tCr): apparent diffusion coefficient of total creatine; MS: multiple sclerosis; HC: healthy controls; CI: confidence interval; *p*: p value; *=$p<0.05$.

Table 3

Thalamic ADC(tCr)									
			MS				HC		
			coefficient	*95% CI*		*p*	*coefficient*	*95% CI*		*p*
case tracts	**SOMATOSENSORY TRACT**	**FA**	261.08	-73.79	595.94	0.119	-141.76	-599	315.47	0.509
		MD	-0.45	-0.77	-0.14	0.008*	0.15	-0.25	0.55	0.421
		AD	-0.32	-0.91	0.28	0.276	0.17	-0.37	0.7	0.501
		RD	-0.52	-0.86	-0.19	0.004*	0.14	-0.38	0.67	0.560
	OPTIC RADIATIONS	**FA**	247.13	-178.82	673.08	0.239	168.64	-115.48	452.76	0.218
		MD	-1.38	-2.55	-0.22	0.022*	-0.38	-1.19	0.44	0.332
		AD	-1.55	-2.72	-0.38	0.012*	-0.31	-1.36	0.75	0.535
		RD	-1.3	-2.5	-0.1	0.035*	-0.41	-1.16	0.34	0.251
	DORSOLATERAL PREFRONTAL TRACT	**FA**	176.88	-319.84	673.60	0.464	107.68	-686.41	901.76	0.771
		MD	-0.84	-1.42	-0.25	0.008*	-0.35	-1.08	0.38	0.310
		AD	-0.88	-1.47	-0.29	0.006*	-0.25	-0.75	0.25	0.292
		RD	-0.81	-1.53	-0.1	0.028*	-0.4	-1.41	0.6	0.393
control tract	**ARCUATE FASCICULUS**	**FA**	41.05	-281.87	363.96	0.792	149.63	-75.32	374.58	0.171
		MD	-0.28	-0.75	0.19	0.223	-0.29	-0.58	0.01	0.055
		AD	-0.42	-0.85	0.01	0.053	-0.32	-0.67	0.03	0.066
		RD	-0.21	-0.74	0.32	0.418	-0.27	-0.61	0.07	0.112

Table 3. Association between thalamic ADC(tCr) and microstructural metrics of tracts: single-tract analysis. Correlations between thalamic ADC(tCr) and DTI-derived metrics (FA, MD, AD, RD) of single tracts in patients with MS. FA: fractional anisotropy; MD: mean diffusivity; AD: axial diffusivity; RD: radial diffusivity, ADC(tCr): apparent diffusion coefficient of total creatine; MS: multiple sclerosis; HC: healthy controls; CI: confidence interval; *p*: p value; *=$p<0.05$.

FIGURE LEGENDS

Figure 1. DW-MRS spectra in one patient with MS. Examples of spectra acquired with and without diffusion weighting (**blue** and **red** lines, respectively) in the deep GM for one single patient with MS. Inset: locations of the volume of interest (VOIs) in the thalami on an axial (a) and sagittal (b) plan. b: b value; ppm: parts per million; tCr: total creatine; tNAA: total N-acetyl-aspartate; MS: multiple sclerosis.

Figure 2. The three thalamo-cortical projections and the arcuate fasciculus. Tracts drawn using TrackVis and overlaid onto sagittal T1-weighted scans of 4 single patients with MS: (a) somatosensory tract (SS, red); (b) optic radiations (OR, green); (c) dorsolateral prefrontal tract (PF, light blue); (d) arcuate fasciculus (AF, purple).

Figure 3. Correlation between thalamic ADC(tCr) and MD of thalamo-cortical tracts: pooled analysis. Margins plot for the linear mixed effect model to test the correlation between thalamic ADC(tCr) and MD of thalamo-cortical tracts in patients with MS (**red**) and HC (**blue**), accounting for age, sex, single tracts and normalized thalamic volume. Results showed a significant and inverse association between tCr diffusivity in the thalamus and MD of thalamo-cortical tracts in patients with MS, but not in HC. MD: mean diffusivity; ADC(tCr): apparent diffusion coefficient of total creatine; CIs: confidence intervals; coef: correlation coefficient; MS: multiple sclerosis; HC: healthy controls.

Figure 4. Correlations between thalamic ADC(tCr) and MD of tracts: single-tract analysis. Scatter plots showing correlations between thalamic ADC(tCr) and MD of single tracts in patients with MS and HC. Linear regressions showed a significant and inverse association between tCr diffusivity in the thalamus and MD of SS, OR, PF tracts. No association was found with the control

tract nor with the tracts of HC. SS: somatosensory tract; OR: optic radiations; PF: dorsolateral prefrontal tract; AF: arcuate fasciculus; MD: mean diffusivity; ADC(tCr): apparent diffusion coefficient of total creatine; coef: correlation coefficient; MS: multiple sclerosis; HC: healthy controls.

Patient with MS

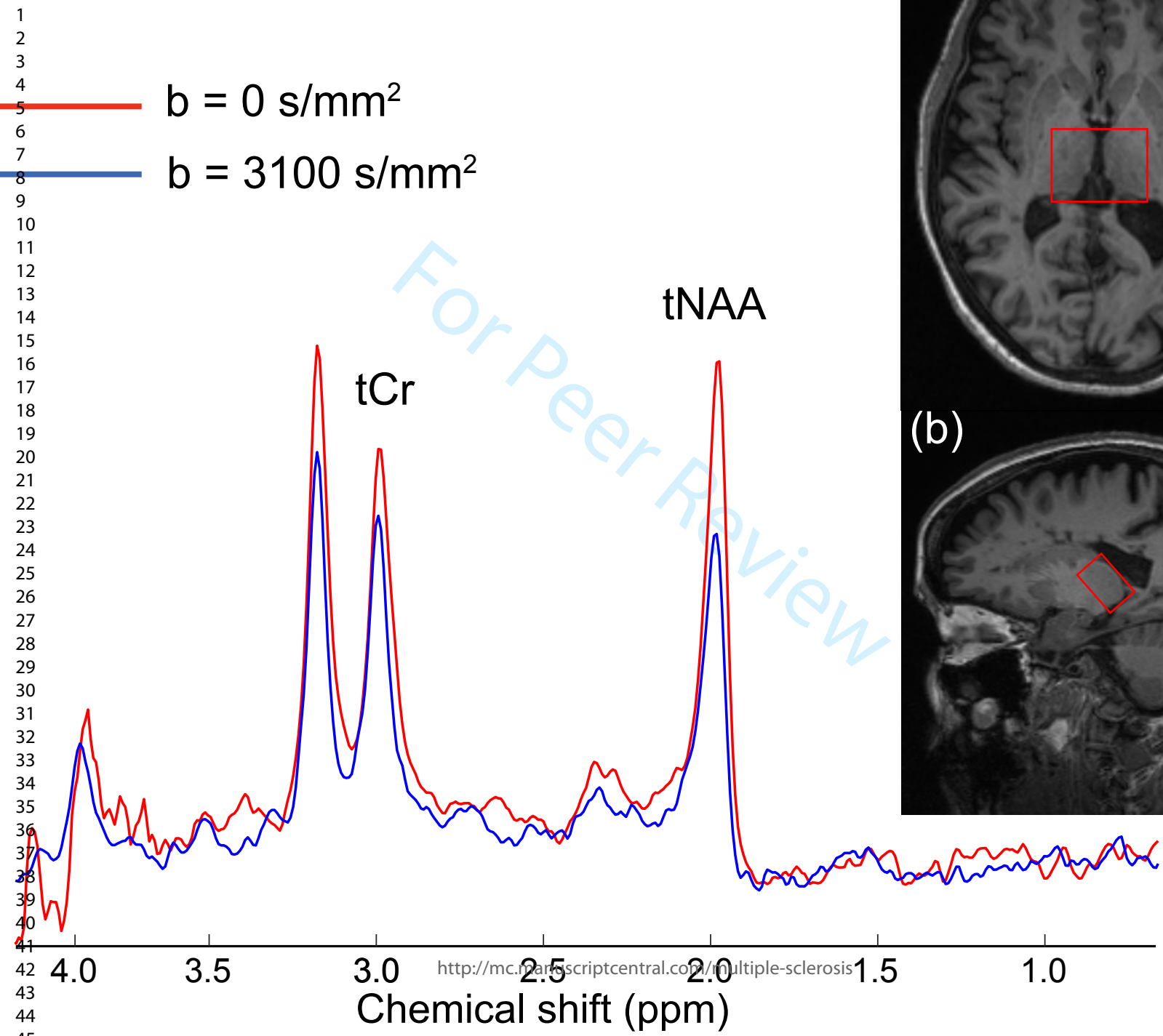

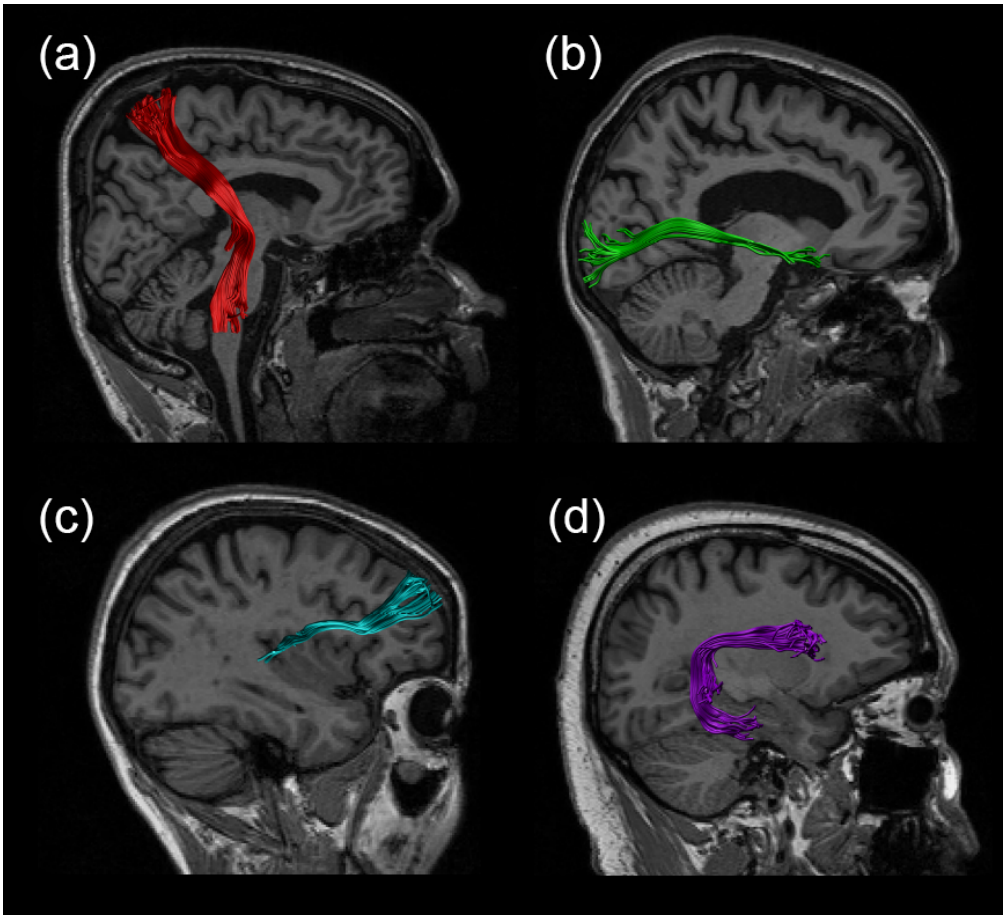

Figure 2. The three thalamo-cortical projections and the arcuate fasciculus. Tracts drawn using TrackVis and overlaid onto sagittal T1-weighted scans of 4 single patients with MS: (a) somatosensory tract (SS, red); (b) optic radiations (OR, green); (c) dorsolateral prefrontal tract (PF, light blue); (d) arcuate fasciculus (AF, purple).

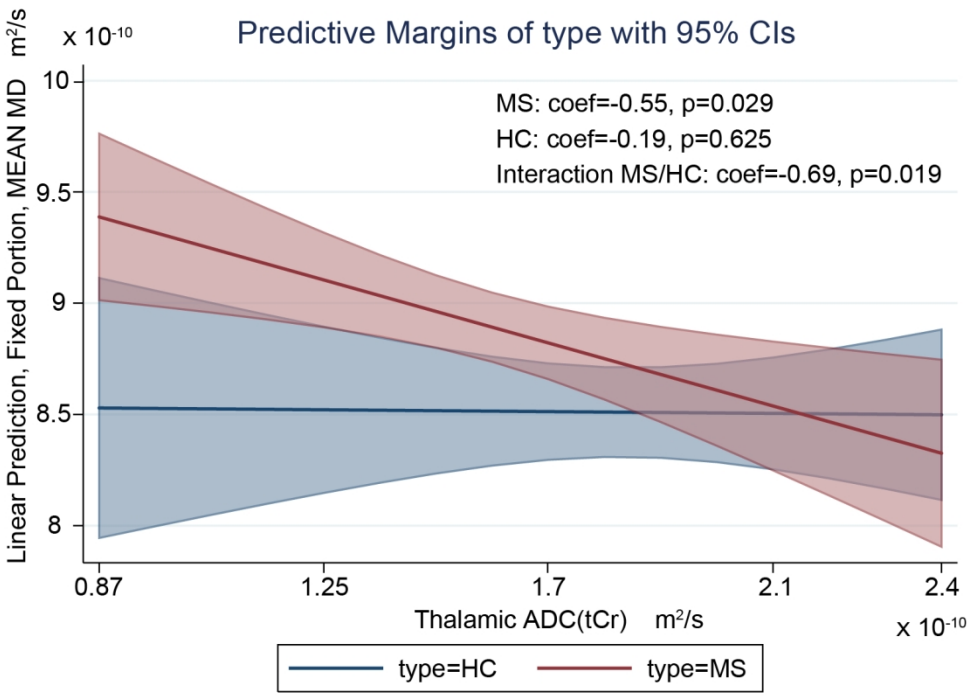

Figure 3. Correlation between thalamic ADC(tCr) and MD of thalamo-cortical tracts: pooled analysis. Margins plot for the linear mixed effect model to test the correlation between thalamic ADC(tCr) and MD of thalamo-cortical tracts in patients with MS (red) and HC (blue), accounting for age, sex, single tracts and normalized thalamic volume. Results showed a significant and inverse association between tCr diffusivity in the thalamus and MD of thalamo-cortical tracts in patients with MS, but not in HC. MD: mean diffusivity; ADC(tCr): apparent diffusion coefficient of total creatine; CIs: confidence intervals; coef: correlation coefficient; MS: multiple sclerosis; HC: healthy controls.

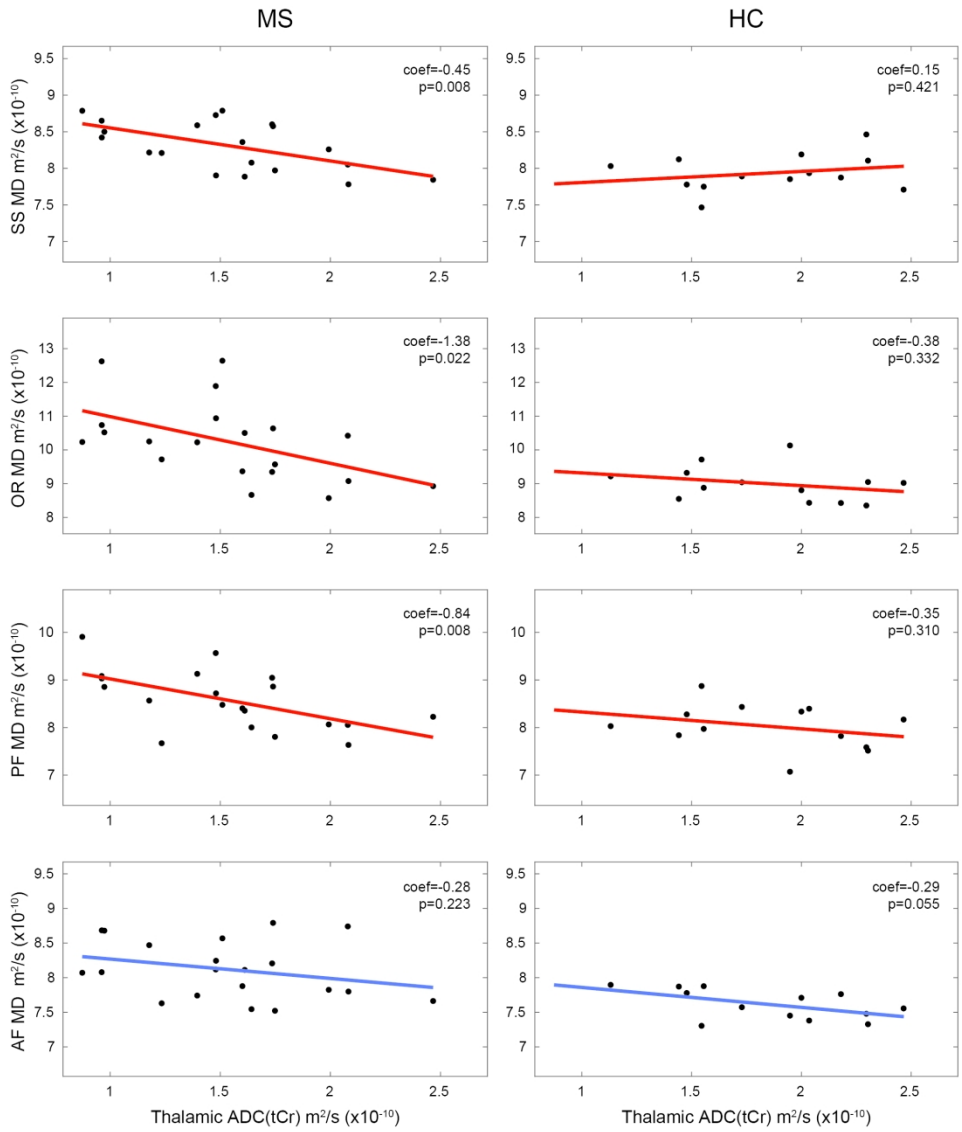

Figure 4. Correlations between thalamic ADC(tCr) and MD of tracts: single-tract analysis. Scatter plots showing correlations between thalamic ADC(tCr) and MD of single tracts in patients with MS and HC. Linear regressions showed a significant and inverse association between tCr diffusivity in the thalamus and MD of SS, OR, PF tracts. No association was found with the control tract nor with the tracts of HC. SS: somatosensory tract; OR: optic radiations; PF: dorsolateral prefrontal tract; AF: arcuate fasciculus; MD: mean diffusivity; ADC(tCr): apparent diffusion coefficient of total creatine; coef: correlation coefficient; MS: multiple sclerosis; HC: healthy controls.

SUPPLEMENTARY MATERIAL S1

MRI protocol

T1-w: field of view in AP, FH, LR directions 240x256x176mm^3, voxel size 1.0x1.0x1.1mm^3, TR/TE 2300ms/2.98ms.

T2-w: field of view 350x350x263mm^3, voxel size 0.9x0.9x3.0mm^3, TR/TE1/TE2 4500/14/83ms.

FLAIR: field of view 230x120x187mm^3, voxel size 0.9x0.9x3.0mm^3, TR/TE 8880/129ms.

DW-MRS: TR=3 cardiac cycles, TE=120ms, spectral width=2kHz, number of points=1024. Diffusion weighting was applied in one direction using a diffusion time of 60ms, gradient duration of 30ms, and a b-value of 3100s/mm^2. For each condition, including a non DW acquisition, 32 spectra were acquired. Water suppression was applied using a frequency selective excitation pulse followed by a dephasing gradient before metabolite excitation. Non-water-suppressed spectra were acquired for eddy current corrections.

DWI: DW directions=50, b=1000s/mm^2 and 1 image at b=0s/mm^2, with the following parameters: TR=7900ms, TE=87ms, flip angle=90°, voxel size=2mm^3.

SUPPLEMENTARY MATERIAL S2.

Tract dissection

Thalamo-cortical tracts:

Two 3D ROIs[1] were drawn on T1-w scans to dissect three pairs of thalamo-cortical tracts: the right and left somatosensory tract, connecting the ventroposterolateral thalamus to the somatosensory cortex (SS); the right and left optic radiation, connecting the lateral geniculate nucleus in the thalami to the primary visual cortex (OR); and the right and left prefrontal tract, connecting the mediodorsal nucleus of the thalamus to the dorso-lateral prefrontal cortex (PF). To dissect each tract, one thalamic seed-region and one cortical target region were manually defined on the axial, coronal, and sagittal planes with reference to FA images at anatomically guided locations (according to known anatomy and available tractography atlases).[2] In particular, for the SS the seed-region was located in the ventroposterolateral thalamus while the target region in the primary sensory cortex of the parietal lobe immediately posterior to the central sulcus. To dissect the OR, the seed region was placed in the lateral geniculate nucleus of the posterior thalamus and the target region in the white matter around the calcarine fissure in the occipital lobe. To dissect the PF, the seed region was located in the mediodorsal nucleus of the anterior thalamus and the target region in the middle frontal gyrus between the superior and inferior frontal sulcus.[3]

Arcuate fasciculus:

The right and left arcuate fasciculus (AF), which were used as "control" tract pair, were dissected taking into account their three components: the fronto-parietal portion running lateral to the projection fibers of the *corona radiata*, the parieto-temporal fibers arching from the temporo-parietal junction around the lateral fissure and continuing downwards into the temporal lobe, and the most lateral component approaching the perisylvian cortex.[2] Three ROIs were employed to obtain the trajectories of the three segments of the arcuate bundle, as previously described.[4] More in detail, a first region of interest (ROI) was defined to encompass the horizontal fibers lateral to the

corona radiata and medial to the cortex in the area corresponding to Talairach z=22-28. Then, two additional and separated regions (frontal and temporal ROIs) were placed, extending beyond the classical limits of Broca's and Wernicke's areas to track the anterior and posterior segments of the bundle.

Supplementary references

1. Catani M, Howard RJ, Pajevic S, Jones DK. Virtual in vivo interactive dissection of white matter fasciculi in the human brain. *Neuroimage* 2002; 17: 77-94.
2. Catani M, Thiebaut de Schotten M. A diffusion tensor imaging tractography atlas for virtual in vivo dissections. *Cortex* 2008; 44: 1105-1132.
3. Klein JC, Rushworth MFS, Behrens TEJ, et al. Topography of connections between human prefrontal cortex and mediodorsal thalamus studied with diffusion tractography. *Neuroimage* 2010; 51: 555-564.
4. Catani M, Jones DK, Ffytche DH. Perisylvian language networks of the human brain. *Ann Neurol* 2005; 57: 8-16.

SUPPLEMENTARY MATERIAL S3

PCr/Cr concentration ratios and diffusivity changes

Phantom experiments were performed in a previous study to assess independently the ADCs of Cr and PCr.[1] The ADC of Cr was found to be about 38% higher than the ADC of PCr (ADC(Cr) = 0.957 $\mu m^2/ms$, ADC(PCr) = 0.680 $\mu m^2/ms$), reflecting the fact that Cr (chemical formula C4H9N3O2, molar mass 131 g/mol) is a smaller molecule than PCr (chemical formula C4H10N3O5P, molar mass 211 g/mol).

Assuming the same ratio between the ADCs of the two molecules in vivo (ADC(Cr) = 0.20 $\mu m^2/ms$ and ADC(PCr) = 0.142 $\mu m^2/ms$), we simulated the normalized signal decay (S/S0) of tCr as a function of the b-value for different fractions of Cr (fCr) and PCr (fPCr = 1- fCr), corresponding to different PCr/Cr concentration ratios (Eq. S1, Figure S1):

$$S/S0 = fCr \cdot \exp(-b \cdot ADC(Cr)) + (1-fCr) \cdot \exp(-b \cdot ADC(Cr)) \qquad (S1)$$

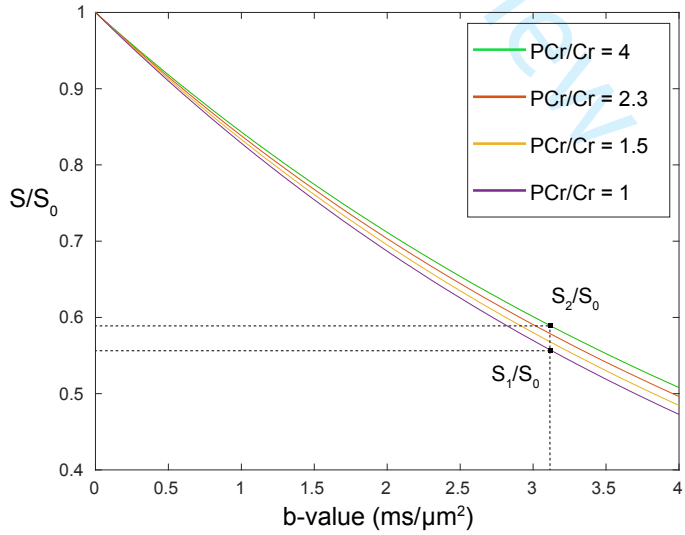

Figure S1. Normalized signal decay of tCr as a function of the b-value for different PCr/Cr ratios. Curves showing the S/S_0 of tCr as a function of the b-value simulated for four different PCr/Cr ratios listed in the top right box.

Black dots indicate the corresponding increase of S/S_0 at the b-value = 3.1 ms/μm^2 for a PCr/Cr ratio increase from 1 to 4. S/S_0: signal decay; S_1/S_0: signal decay when PCr/Cr ratio = 1; S_2/S_0: signal decay when PCr/Cr ratio = 4; PCr: phosphocreatin; Cr: creatin.

In our study, we employed one b-value b = 3.1 ms/μm^2, and the ADC of tCr was calculated as

$$ADC(tCr) = -\ln(S/S0)/b \qquad (S2)$$

According to the plots in Figure S1:

S1/S0 = 0.56 corresponds to the signal at b = 3.1 ms/μm^2 obtained for fractions fPCr = 0.5 and fCr = 0.5 (PCr/Cr = 1), and S2/S0 = 0.59 corresponds to the signal at the same b-value obtained for fractions fPCr = 0.8 and fCr = 0.2 (PCr/Cr = 4).

Using equation (S2) the estimated ADC(tCr) for the two cases are:

ADC(tCr) = 0.19 μm^2/ms for fPCr = 0.5 and fCr = 0.5, and

ADC(tCr) = 0.17 μm^2/ms for fPCr = 0.8 and fCr = 0.2,

which corresponds to a decrease in ADC(tCr) of 10%, a bit lower than that observed in our study (17%).

Supplementary references

1. Branzoli F, Techawiboonwong A, Kan H, et al. Functional diffusion-weighted magnetic resonance spectroscopy of the human primary visual cortex at 7T. *Magn Reson Med* 2013; 69: 303-309.